Paper

Adhesion Control in Low-Speed Region with Considering Low-Resolution Pulse Generator

Meifen Cao* Member
Keiichi Takeuchi** Member
Takemasa Furuya* Student Member
Atsuo Kawamura* Member

In the proposed adhesion control methods with sensors, the wheel speed is required for the tractive force estimation. However, in the railway field, the pulse generator (PG) used for the wheel speed measurement is attached on the main motor and with only 60 pulse-per-revolution (ppr). Therefore, when the train is in the low-speed region, the speed value cannot be obtained in each control period. To solve this problem, the adhesion control in low-speed region with considering the low-resolution PG is proposed in this paper. In this control method, a disturbance-instantaneous-speed observer is designed to (1) estimate the instantaneous wheel speed from the motor torque and the corrected tractive torque, (2) correct the estimated tractive torque when the real speed signal is measured from PG. The simulation and experiment verification results of the effectiveness of the proposed adhesion control with the instantaneous wheel speed estimation are reported.

Keywords: Adhesion control, Low-speed region, Low resolution, Pulse generator (PG), Disturbance-instantaneous-speed observer

1. Introduction

The improvement of the speed adjustment capability is mentioned as one of the means which increase transport capacity while maintaining the safety of a high speed railway system. Increasing the traction and the brake force is mentioned as the general technique for improving the acceleration or deceleration capability. However, by increasing the motor torque simply to increase traction and brake force, according to the adhesion phenomenon between wheels and rails, the slip phenomenon occurs and the speed adjustment capability can not be improved.

When a traction torque is added to a running wheel, the traction force transmitted in the tangent direction of the contact surface of the wheel and the rail will increase with the slip increasing, and will be saturated under a certain slip. The saturation point is called "adhesion limit". Furthermore, if the traction torque is increased continually, the slip will increase rapidly and the train will fall into the slip state rapidly. This phenomenon is called "adhesion phenomenon" in the railway field [1].

Now, several methods such as the sprinkling sand and the injecting ceramic particles methods, are adopted as a physical technique for acquiring the necessary traction force required by traction or braking force. On the other hand, several control methods have been proposed. In these methods, the tractive force is estimated by a disturbance observer and the motor torque is controlled to drive a train by the maximum tractive force during acceleration, deceleration or a sudden change of the rail surface condition. These methods which use the adhesion phenomenon effectively are called "adhesion control" or "maximum tractive force control".

In these adhesion control methods [2]~[5], the wheel speed is required for the tractive force estimation. However, the mainstream of the present railway vehicles is the inverter controlled vehicles. In such vehicles, the wheel speed is measured by the 60 pulse-per-revolution (ppr) pulse generator (PG) attached in the main motor [1]. Because of the low resolution of the PG, the speed information cannot be acquired in every control period of DSP when the train is in low-speed region.

An adhesion control in low-speed region with a disturbance-instantaneous-speed observer [6] is proposed in this paper. With this method the instantaneous wheel speed in low-speed region can be estimated by the proposed disturbance-instantaneous-speed observer. The effectiveness of the proposed adhesion control in low-speed region has been verified by simulations and experiments.

2. Review of the Adhesion Control

The adhesion control (or the maximum tractive force control), in which the motor torque is controlled to drive vehicles by maximum tractive force, has been proposed by the authors group until now [2] [3] [7] [8]. According to the "adhesion phenomenon", the steepest gradient

* Yokohama National University
79-5, Tokiwadai, Hodogaya-ku,Yokohama 240-8501
** Railway Technical Research Institute
2-8-38, Hikari-cho, Kokubunji-shi, Tokyo 185-8540

method can be used to approach the "adhesion limit" [2] (the peaks in Fig. 1).

In our proposed control method, a one-axle model shown in Fig. 2 [3] is considered.

This model is expressed as follows:

$$J_n \frac{d\omega}{dt} = T_e - T_L - B\omega, \quad \cdots\cdots (1)$$

$$M \frac{dv}{dt} = F_{ad} - cv^2, \quad \cdots\cdots (2)$$

$$F_{ad} = \mu M g, \quad \cdots\cdots (3)$$

$$T_L = F_{ad}\, r, \quad \cdots\cdots (4)$$

$$v_{slip} = \omega r - v, \quad \cdots\cdots (5)$$

where T_e is the motor torque, T_L is the tractive force torque, B is the viscosity resistance coefficient, J_n is the moment of inertia, ω is the wheel (angular) speed, M is the mass of the train, v is the train speed, F_{ad} is the tractive force, c is the air resistance coefficient, μ is the tractive force coefficient, g is the gravitational constant, r is the radius of the wheel, and v_{slip} is the slip speed.

An example of the characteristics between μ and v_{slip} is shown in Fig. 1, as defined in (1) $\sim$ (5). v_{slip} and F_{ad}(or μ) is positive during the acceleration and negative during the deceleration. Moreover, the region at that the absolute value of the slip speed is smaller than the slip speed of the "adhesion limit" is called "creep region" and the region at that the absolute value of the slip speed is larger than the absolute value of the "adhesion limit" is called "slip region" [1].

The tractive force F_{ad} between the wheel and the rail is estimated by a disturbance observer at first. Then the

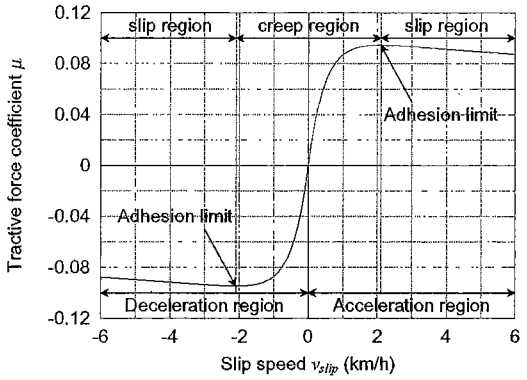

Fig. 1. Adhesion characteristic used for both acceleration and deceleration.

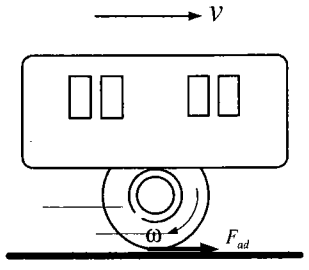

Fig. 2. One axle model of driving wheel.

differential of the estimated tractive force and the differential of the slip speed are used to find the slip speed reference at which the tractive force will reach the peak. Then the motor torque will be controlled by the wheel speed reference which can be derived from the slip speed reference. The slip reference generation algorithm can be shown as below:

Slip reference generation algorithm

(1) $\frac{d\hat{F}_{ad}}{dv_{slip}}$ is calculated by $\frac{d\hat{F}_{ad}}{dt} / \frac{dv_{slip}}{dt}$, where $\hat{F}_{ad}$ is the estimated tractive force.

(2) slip reference is calculated by $v_{slip_{ref}}(k+1) = v_{slip_{ref}}(k) + \alpha \frac{d\hat{F}_{ad}}{dv_{slip}}$, where the value of α is a constant.

(3) return to (1).

However, the above method has a difficult point that the system will become unstable when the differential of slip speed is approaching zero. As a solution, the new slip reference generation rule which uses the second degree differential of slip speed was proposed [3]. The new control rule controls the motor torque with assuming that the motor torque balances with the maximum tractive force when the second degree differential of the slip speed is approaching zero.

It is verified that the method using the second degree differential of slip speed is effective in simulation. However, when it is used to an experiment or a real train, the new problem referred to as how correctly the second degree differential can be computed will occur. As a solvent for this problem, the algorithm was improved as follows:

Improved slip reference generation algorithm

(1) $\frac{d\hat{F}_{ad}}{dv_{slip}}$ is calculated by $P(k) = \mathrm{sign}(\frac{dv_{slip}}{dt}) \frac{\frac{d\hat{F}_{ad}}{dt}}{\varepsilon_0 + |\frac{dv_{slip}}{dt}|}$, where ε_0 is a very small positive number.

(2) $Q(k)$ is the value of $P(k)$ passed by an LPF

(3) $v_{slip_{ref}}(k+1) = v_{slip_{ref}}(k) + \alpha Q(k)$, where α is variable according to $Q(k)$ as $\alpha = \alpha_{min} \frac{Q_{max} - |Q(k)|}{Q_{max}} + \alpha_{max} \frac{|Q(k)|}{Q_{max}}$, and α_{min}, α_{max}, and Q_{max} are constants.

(4) return to (1).

3. Proposal for the Adhesion Control in Low-Speed Region with the Disturbance-Instantaneous-Speed Observer

In the above-mentioned adhesion control schemes, the wheel speed is required. However, the 60 ppr PG attached in the main motors of the inverter controlled vehicles are used mainly in the present railway system. When a train is in low-speed region, the pulse period T_{smp1} of PG is much longer than the DSP control period T_{smp2} as shown in Fig. 3. Thus, the speed information cannot be acquired for every DSP control period [9] [10].

In this section, a disturbance-instantaneous-speed ob-

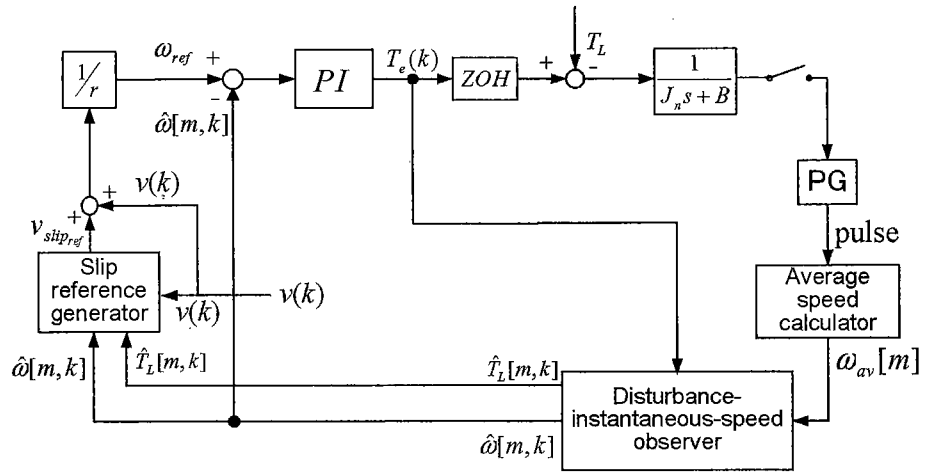

Fig. 4. Block diagram of the proposed adhesion control.

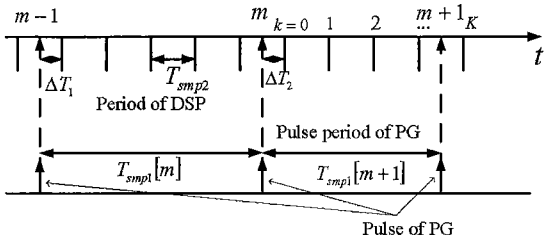

Fig. 3. Timing chart in low-speed region [6].

server ((16) $\sim$ (19)) is derived and the adhesion control system which includes the wheel speed estimation in low-speed region is proposed as shown in Fig. 4.

Let the tractive torque T_L be a disturbance. A disturbance observer can be constructed from (1), and the following state equations are derived.

$$\frac{d}{dt}\begin{bmatrix}\dot{T}_L\\ T_L\\ \omega\end{bmatrix}=\begin{bmatrix}0 & 0 & 0\\ 1 & 0 & 0\\ 0 & -\frac{1}{J_n} & -\frac{B}{J_n}\end{bmatrix}\begin{bmatrix}\dot{T}_L\\ T_L\\ \omega\end{bmatrix}+\begin{bmatrix}0\\ 0\\ \frac{1}{J_n}\end{bmatrix}T_e \quad \cdots\cdots (6)$$

$$y(t)=\begin{bmatrix}0 & 0 & 1\end{bmatrix}\begin{bmatrix}\dot{T}_L\\ T_L\\ \omega\end{bmatrix} \quad \cdots\cdots (7)$$

A low-order disturbance observer can be constituted by the Gopinath method from (6) and (7).

$$\frac{d}{dt}\begin{bmatrix}z_1\\ z_2\end{bmatrix}=\mathbf{D}\begin{bmatrix}z_1\\ z_2\end{bmatrix}+\mathbf{E}\omega+\mathbf{J}T_e, \quad \cdots\cdots (8)$$

$$\begin{bmatrix}\hat{\dot{T}}_L\\ \hat{T}_L\end{bmatrix}=\begin{bmatrix}1 & 0\\ 0 & 1\end{bmatrix}\begin{bmatrix}z_1\\ z_2\end{bmatrix}+(-\mathbf{L})\omega, \quad \cdots\cdots (9)$$

where $\mathbf{D}$, $\mathbf{E}$, $\mathbf{J}$, $\mathbf{L}$ can be calculated from the poles of the observer and J_n, B of the motor, and z_1, z_2 are the state variables of the observer, and $\hat{T}_L$, $\hat{\dot{T}}_L$ are the estimation values of the disturbance torque and its differential.

The discretization results of (8) and (9) are shown as,

$$\begin{bmatrix}z_1(n)\\ z_2(n)\end{bmatrix}=\mathbf{D_z}\begin{bmatrix}z_1(n-1)\\ z_2(n-1)\end{bmatrix}+\mathbf{B_z}\begin{bmatrix}\omega(n-1)\\ T_e(n-1)\end{bmatrix}, \quad (10)$$

where n is an integer variable ($n=1,2,3,...$).

$$\begin{bmatrix}\hat{\dot{T}}_L(n)\\ \hat{T}_L(n)\end{bmatrix}=\begin{bmatrix}1 & 0\\ 0 & 1\end{bmatrix}\begin{bmatrix}z_1(n)\\ z_2(n)\end{bmatrix}+\mathbf{L_z}\omega(n-1), \cdots (11)$$

where $\mathbf{D_z}$, $\mathbf{B_z}$ and $\mathbf{L_z}$ can be derived from $\mathbf{D}$, $\mathbf{E}$, $\mathbf{J}$, $\mathbf{L}$ and sampling time T which is DSP period T_{smp2} shown in Fig. 3.

It is assumed that ΔT_1 and ΔT_2 in Fig. 3 can be measured here.

Equation (10) and (11) are written to (12) and (13) to fit to Fig. 3,

$$\begin{bmatrix}z_1[m,k]\\ z_2[m,k]\end{bmatrix}=\mathbf{D_z}\begin{bmatrix}z_1[m,k-1]\\ z_2[m,k-1]\end{bmatrix}+\mathbf{B_z}\begin{bmatrix}\omega[m,k-1]\\ T_e[m,k-1]\end{bmatrix}, \cdots\cdots (12)$$

$$\begin{bmatrix}\hat{\dot{T}}_L[m,k]\\ \hat{T}_L[m,k]\end{bmatrix}=\begin{bmatrix}1 & 0\\ 0 & 1\end{bmatrix}\begin{bmatrix}z_1[m,k]\\ z_2[m,k]\end{bmatrix}+\mathbf{L_z}\omega[m,k-1], \cdots\cdots (13)$$

where m and k are defined in Fig. 3.

In (12) and (13), because the wheel speed $\omega[m,k-1]$ cannot be obtained from PG in the low-speed region, the estimation value $\hat{\omega}[m,k-1]$ is used. The disturbance observer can be represented in (14) and (15).

$$\begin{bmatrix}z_1[m,k]\\ z_2[m,k]\end{bmatrix}=\mathbf{D_z}\begin{bmatrix}z_1[m,k-1]\\ z_2[m,k-1]\end{bmatrix}+\mathbf{B_z}\begin{bmatrix}\hat{\omega}[m,k-1]\\ T_e[m,k-1]\end{bmatrix} \cdots\cdots (14)$$

$$\begin{bmatrix}\hat{\dot{T}}_L[m,k]\\ \hat{T}_L[m,k]\end{bmatrix}=\begin{bmatrix}1 & 0\\ 0 & 1\end{bmatrix}\begin{bmatrix}z_1[m,k]\\ z_2[m,k]\end{bmatrix}+\mathbf{L_z}\hat{\omega}[m,k-1] \cdots\cdots (15)$$

The wheel speed can be estimated in every DSP control period by

$$\hat{\omega}[m,k]=\hat{\omega}[m,k-1]$$

$$+\frac{T_{smp2}}{2}\left(\frac{T_e[m,k]+T_e[m,k-1]}{J_n}\right) -\frac{T_{smp2}}{2}\left(\frac{\hat{T_{Lc}}[m,k]+\hat{T_{Lc}}[m,k-1]}{J_n}\right). \quad \cdots\cdots (16)$$

This equation can be derived from (1) with the disturbance estimation value $\hat{T_L}$ acquired from the disturbance observer, where $\hat{T_{Lc}}$ is the corrected $\hat{T_L}$ by (19).

At time m, the new average speed $\omega_{av}[m]$ is calculated by interval between the pulses measured from PG. Here it is considered that the speed estimation error is mainly caused from the discretization error of the disturbance observer. We propose the following scheme as the correcting method of $\hat{T_L}$ which is obtained from the disturbance observer. Moreover, we propose that the wheel speed at $[m,k]$ can be estimated from (16) with $\hat{T_{Lc}}$ corrected by (19).

$$\Delta\omega[m,k] \triangleq \hat{\omega}[m,k-1]-\omega_{av}[m], \quad \cdots\cdots (17)$$

$$\Delta T_L[m,k] \triangleq \frac{K_c J_n}{T_{smp2}}\Delta\omega[m,k], \quad \cdots\cdots (18)$$

$$\hat{T}_{Lc}[m,k]=\hat{T}_L[m,k]+\Delta T_L[m,k]\frac{T_{smp2}}{T_{smp1}[m]}, \quad \cdots\cdots (19)$$

where K_c is the correction gain, and $\omega_{av}[m]$ can be calculated by

$$\omega_{av}=\frac{2\pi}{NP\cdot T_{smp1}}, \quad \cdots\cdots (20)$$

$$T_{smp1}=\Delta T_1+K\cdot T_{smp2}-\Delta T_2, \quad \cdots\cdots (21)$$

where NP is the product of the gear ratio and the resolution of PG ($NP=128$ in this paper, it will be explained more detailed in section 5), K is the ratio of the pulse period T_{smp1} and the DSP period T_{smp2}.

4. Simulation Verification of the Control Performance of the Proposal System

The simulation for verifying the validity of the proposed method was performed under conditions below:

- The wheel speed was accelerated from 0 km/h; it was changed to the deceleration preparation state at $t=20$ s, and it was in the deceleration state from $t\approx 22.5$ s.
- The rail condition was changed from "condition 1" to "condition 2" at $t=0.8$ s and $t=12$ s during acceleration, and $t=36$ s during deceleration.
- The rail condition was changed from "condition 2" to "condition 1" at $t=3.0$ s and $t=15$ s during acceleration.

The parameters used in the simulations are shown in Table 1, where J_n and B are measured values of the experiment equipment [7].

When the pulse period T_{smp1} was larger than the control period T_{smp2} ($T_{smp1}>T_{smp2}$, in the low-speed region), ω was estimated by (16) and $\hat{T_L}$ was corrected by (19).

Fig. 5 shows the wheel speed and the train speed during the whole acceleration and deceleration period. Fig. 6 and Fig. 7 show that the instantaneous wheel speed was estimated successfully in low-speed region. Fig. 8 and Fig. 9 show the used tractive coefficient during acceleration and deceleration. From Fig. 8 and Fig. 9 it can be known that even the rail condition was changed suddenly in low-speed region the proposed adhesion control was working well and the slip was controlled successfully. Fig. 10 shows the slip speed during the whole acceleration and deceleration period.

At $t=0.8$ s, the slip speed increased suddenly (point (1) in Fig. 8 and Fig. 10) with the sudden change of the tractive condition, and increased continually (point (1) → point (2) in Fig. 8 and Fig. 10). Because it was still in the "creep region" (the region at the left side of the "adhesion limit" shown in Fig. 8) the slip reference was increased continually by the proposed control algorithm.

At $t=12$ s and $t=36$ s, the slip speed increased at a moment (point (3) in Fig. 8 and Fig. 10, point (6) in Fig. 9 and Fig. 10) with the sudden change of the tractive condition, and decreased after that (point (3) → point (4) in Fig. 8 and Fig. 10, point (6) → point (7) in Fig. 9 and Fig. 10). Because it was in the "slip region" (the region at the right side of the "adhesion limit" shown in Fig. 8 and at the left side of the "adhesion limit" shown in Fig. 9) the slip reference was decreased to prevent heavy slipping or skidding by the proposed control algorithm.

The judgment of the stop instant is difficult in the very low-speed region ($v_{wheel}<0.1$ (km/h) is equivalent of $\omega<5$ rpm) of Fig. 7, because there is no speed signal (no pulse from PG) near the stopping point.

Table 1. The parameters used in the simulations and the experiments.

Moment of inertia J_n	0.021 (kg·m^2)
Viscosity resistance coefficient B	0.007 (N·m·sec/rad)
Air resistance coefficient c	0.0 (sec^2/m^3)
Weight of axle M	51 (kg)
Radius of the vehicle-side-wheel r	53.75 (mm)
Product of the gear ratio and the resolution of PG NP	128
DSP control period T_{smp2}	0.1 (msec)
Correction gain K_c	2

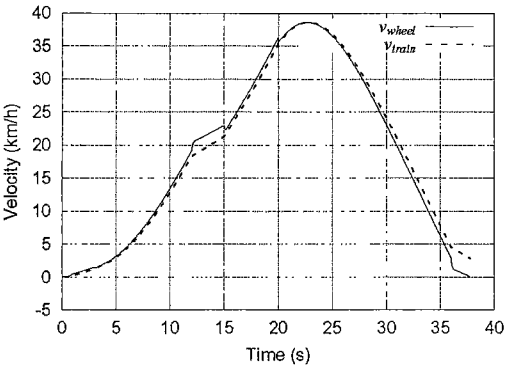

Fig. 5. The speed of wheel and train.

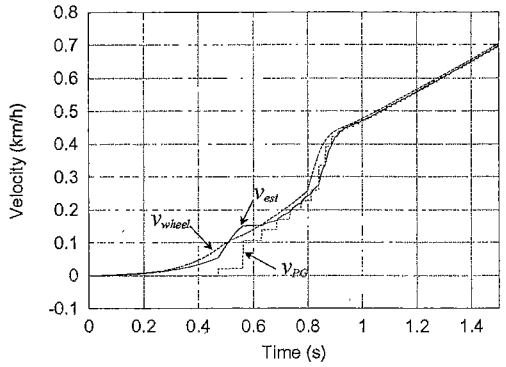

Fig. 6. The real, estimated and measured wheel speed (in low-speed region during acceleration).

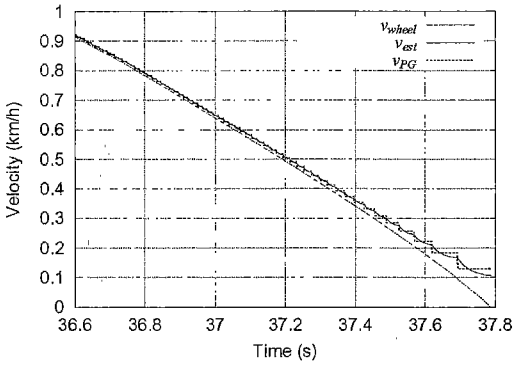

Fig. 7. The real, estimated and measured wheel speed (in low-speed region during deceleration).

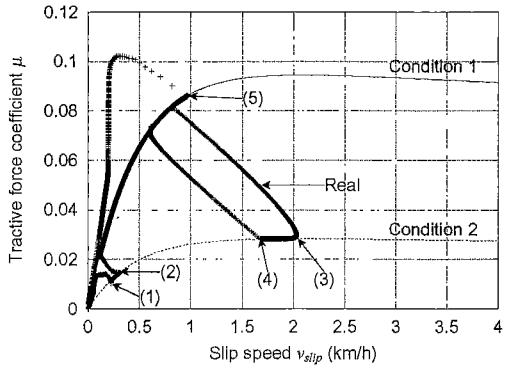

Fig. 8. The used tractive coefficient during acceleration.

5. Experiment Verification of the Control Performance of the Proposal System

The experiment for verifying the validity of the proposal control method was performed with the tractive force measurement equipment developed at our laboratory [11]. This equipment can be used to imitate the acceleration state of a real train by controlling the rail-side-wheel and the vehicle-side-wheel [12]. The perpendicular load between the wheel and the rail, which is equivalent to vehicle weight, can also be set up arbitrarily. The proposal system configuration of the experiment is shown in Fig. 11, where the block "C" is the coefficient for converting a linear into an angular (a rotational) motion. The axle load was set to 500 N in the experiment.

Moreover, a wet rail condition can be imitated by injecting water to both the wheels in this equipment; however, it is difficult to change the rail condition during acceleration. Thus, the experiment was performed only in the dry rail condition. In the experiment, (22) is used as the model of the vehicle-side-wheel, (23) is used as the model of the rail-side-wheel, and (24) is used as the tractive force model.

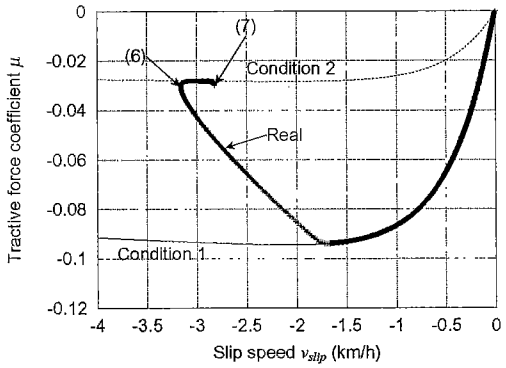

Fig. 9. The used tractive coefficient during deceleration.

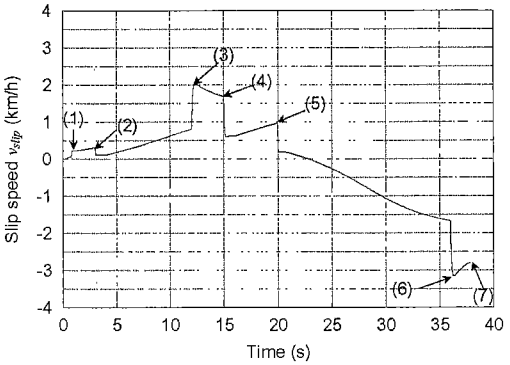

Fig. 10. The slip speed during acceleration and deceleration.

$$J_n \frac{d\omega}{dt} = T_e - F_{ad} r - B\omega, \quad \cdots\cdots\cdots\cdots\cdots (22)$$

$$\frac{dv}{dt} = \frac{\hat{F}_{ad}}{M}, \quad \cdots\cdots\cdots\cdots\cdots\cdots\cdots\cdots\cdots (23)$$

$$F_{ad} = \mu M g, \quad \cdots\cdots\cdots\cdots\cdots\cdots\cdots\cdots\cdots (24)$$

where estimated tractive force $\hat{F}_{ad}$ and estimated instantaneous speed $\hat{\omega}$ in low-speed region were obtained by the disturbance-instantaneous-speed observer described above.

In this equipment, the rail-side-wheel and the vehicle-side-wheel are driven by the induction motors, respectively, and the 1024 ppr PG is equipped in each induction motor. In a real train, the wheel speed is measured from the PG of the traction motors in the motor vehicles and the train speed is measured from the PG attached in the trailer. Moreover, since the gear ratio of a wheel and its motor is usually 1:3 in the case of Shinkansen, the pulse signal from the vehicle-side-PG should be divided by 8 (means the resolution of the PG is set to $1024/8 = 128$ ppr) to imitate the case of Shinkansen (the resolution of the PG is 3×60 ppr $= 180$ ppr in the case of Shinkansen).

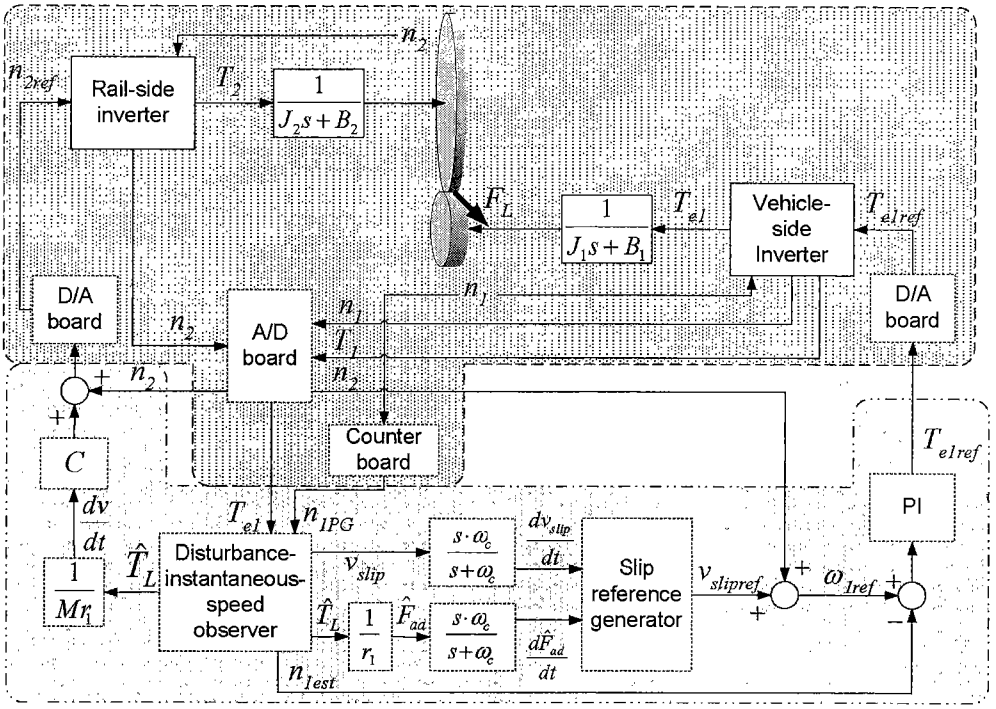

Fig. 11. Experimental system for adhesion control in low-speed region.

In the experiment, the vehicle-side-wheel and the rail-side-wheel speed references were generated by the proposed adhesion control system from zero speed. The vehicle-side-motor torque reference was generated by PI controller. When $v_{train} < 5\,(\mathrm{km/h})$, the vehicle-side-wheel instantaneous speed values between the pulses of PG were estimated by the proposed disturbance-instantaneous-speed observer.

The experimental results of the acceleration state with the proposed disturbance-instantaneous-speed observer are shown in Fig. 12 and Fig. 13. Fig. 12 shows that (1) the wheel speed in low-speed region was estimated successfully, (2) the correction is working when the speed information from PG is updated, and the estimated wheel speed value is gradually approaching to the real speed obtained from PG. Fig. 13 shows that the driving torque and the tractive force torque were computed correctly in the low-speed region by the proposed adhesion control.

In addition, since it is impossible to change the motor torque to reverse direction during acceleration with this equipment at present, the experiment about deceleration can not be reported in this paper.

6. Conclusions

The adhesion control system which estimates the wheel speed between pulses from PG in low-speed region by the disturbance-instantaneous-speed observer is proposed. The effectiveness of the proposed adhesion control were verified by simulation and experiments. As the results, the instantaneous wheel speed was estimated successfully in low-speed region by the proposed scheme; and the proposed adhesion control was working well and the slip was controlled successfully even when the rail condition was changed suddenly in low-speed region.

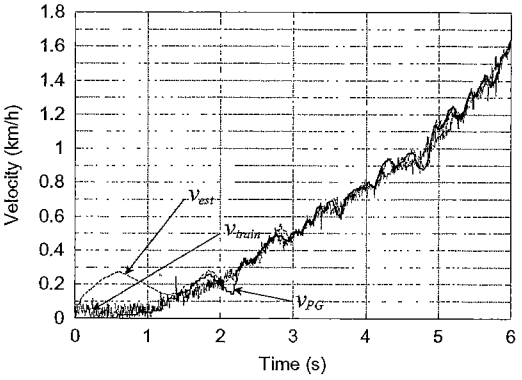

Fig. 12. The real, estimated vehicle-side-wheel and rail-side-wheel speed in the experiment.

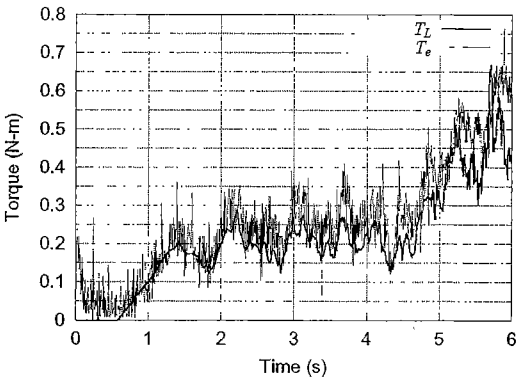

Fig. 13. The driving motor torque and the tractive force torque in the experiment.

Acknowledgment

This research was supported by the Program for Promoting Fundamental Transport Technology Research

from the Corporation for Advanced Transport & Technology (CATT).

(Manuscript received Aug. 6, 2002,
revised March 11, 2003)

References

(1) I.C. of Adhesion Control in Railway System: "Adhesion control technology of railway vehicle," Tech. Rep. 673, IEE of Japan, (1998) (in Japanese)

(2) Y. Ishikawa and A. Kawamura: "Maximum adhesive force control in super high speed train," in *PCC-97*, pp.951–954 (1997)

(3) Y. Takaoka and A. Kawamura: "Disturbance observer based adhesion control for shinkansen," in *AMC2000*, pp.169–174 (2000)

(4) A. Yamanaka and T. Watanabe: "Anti-slip readhesion control presuming adhesion force," *T.IEE Japan*, Vol.119-D, pp.243–253, Feb. (1999) (in Japanese)

(5) K. Ohishi, Y. Ogawa, K. Nakano, I. Miyashita, and S. Yasukawa: "An approach of anti-slip readhesion control of electric motor coach based on first order disturbance observer," *T. IEE Japan*, Vol.120-D, pp.382–389, March (2000) (in Japanese).

(6) Y. Hori and K. Ohnishi: *Applied Control Systems*. Maruzen Co., (1998) (in Japanese)

(7) A. Kawamura, K. Takeuchi, T. Furuya, Y. Takaoka, K. Yoshimoto, and M. Cao: "Measurement of the tractive force and the new adhesion control by the newly developed tractive force measurement equipment," in *Proceedings of the Power Conversion Conference-Osaka 2002*, pp.879–884 (2002)

(8) A. Kawamura, M. Cao, K. Takeuchi, and T. Furuya: "Measurement of the tractive force in the creep region and maximum adhesion force control of high speed railway systems," in *WCRR2001*, pp., No.208 in CD–ROM (2001)

(9) M. Cao, K. Takeuchi, T. Furuya, and A. Kawamura: "Adhesion control performance in low speed region and experiment verification with considering low resolution pulse sensor," in *Papers of Joint Technical Meeting on Transportation and Electric Railway, and Linear Drives, IEE Japan*, pp., TER–01–31 (2001) (in Japanese)

(10) M. Cao, K. Takeuchi, T. Furuya, and A. Kawamura: "Adhesion control in low-speed region and experiment verification with considering low-resolution pulse generator," in *Proceedings of the Power Conversion Conference-Osaka 2002*, pp.873–878 (2002)

(11) A. Kawamura, K. Takeuchi, Y. Takaoka, K. Yoshimoto, T. Furuya, and M. Cao: "Measurement of tractive force and the new maximum tractive force control by the newly developed tractive force measurement equipment," in *Papers of Joint Technical Meeting on Transportation and Electric Railway, and Linear Drives, IEE Japan*, pp., TER–01–32 (2001) (in Japanese).

(12) Y. Takaoka and A. Kawamura: "Maximum adhesion control for electric cars with consideration the quantization of motor shaft sensor that emits sixty pulse per revolution," in *Papers of Technical Meeting on Industrial Instrumentation and Control, IEE Japan*, pp., IIC–01–5 (2001) (in Japanese).

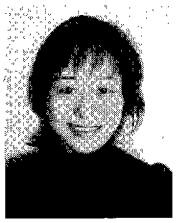

Meifen Cao (Member) received her M.E degrees in 1987 from the Department of Electrical Engineering, Shanghai JiaoTong University. She has been an assistant professor from the same year and a lecturer from 1989 at the same university. She received her PhD degree in 1999 from the Department of Electrical Engineering, Yokohama National University. Until April of 2002 she has been a researcher of the Corporation for Advanced Transport & Technology (CATT). Now she is a researcher of Japan Society for the Promotion of Science. Her research areas are adhesion control of high speed railway, robotics and power electronics.

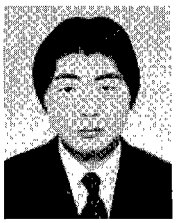

Keiichi Takeuchi (Member) was born in 1977. He received his B.E and M.E degrees in 2000 and 2002 from the Department of Electrical Engineering, Yokohama National University. Since April of 2002, he joined Railway Technical Research Institute. His research topics are adhesion control of high speed railway and etc.

Takemasa Furuya (Student Member) was born in 1978. He received his B.E degree in 2001 from the Department of Electrical Engineering, Yokohama National University. Since April of 2002, he is a master student of the same university. His research topics are adhesion control of high speed railway and etc.

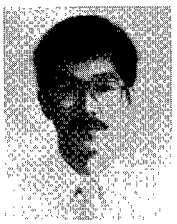

Atsuo Kawamura (Member) was born in Yamaguchi Prefecture, Japan, in December 1953. He received the B.S.E.E., M.S.E.E., and Ph.D. degrees in electrical engineering from the University of Tokyo, Tokyo, Japan, in 1976, 1978, and 1981, respectively. In 1981 he joined the Department of Electrical and Computer Engineering at the University of Missouri-Columbia as a Postdoctoral Fellow, and was an Assistant Professor there from 1983 through 1986. He joined the Department of Electrical and Computer Engineering Yokohama National University, Yokohama, Japan in 1986 as an associate professor, and in 1996 he became a professor. His interests are in power electronics, digital control, electric vehicles, robotics, train traction control and so on. He received the IEEE IAS Transaction Prize Paper Award in 1988, and also the Prize Paper Award of IEE of Japan in 1996. He was the conference chairperson of the IEEE/IAS and IEEJ/IAS joint Power Conversion Conference (PCC-Yokohama) in 1993. He served as the technical program chairman of Power Electronics Specialist Conference in 1998 (PESC'98) and also the workshop on Advanced Motion Control in 2000 (AMC2000). He was an associate editor of IEEE Power Electronics Transactions from1995 to 2000. Dr. Kawamura is an IEEE Fellow, a member of Robotics Society of Japan, the Institute of Electronics, Information and Communication Engineers, the Society of Instrument and Control Engineering and so on.